Seasonality in the Vertical Structure of Long-Term Temperature Trends Over North America

Natalie Thomas[1†], Sumant Nigam [1*], and Vishal Ravi[2]

[1]Department of Atmospheric and Oceanic Science, University of Maryland, College Park, Maryland, United States
[2]Department of Materials Science and Engineering, University of California Berkeley, Berkeley, California, United States

[Original manuscript received 3 May 2020; accepted 31 October 2020]

ABSTRACT *The surface warming of northern continents during the twentieth century is not uniform across seasons. Surface warming is particularly pronounced over northwestern Canada, where winter trends are much larger than summer ones. The upper-air temperature trends over the region are analyzed in three radiosonde datasets from 1958 to 2012 to assess their seasonal structure. The seasonal variation of upper-air trends can provide insights into the dynamical and thermodynamical processes generating these trends, including warming at the surface. The focus is not on the canonical structure of secular (i.e., long-term) trends—tropospheric warming and stratospheric cooling—but its seasonal variation. We find the boreal winter-minus-summer difference in trends over northwestern Canada to be positive and large in the lower troposphere (*$p \gtrsim$ *500 hPa) and lower stratosphere (50 hPa* $\lesssim p \lesssim$ *150 hPa); it is largest at the surface and smallest at the tropopause. The decreasing seasonality of the tropospheric trend with height supports the attribution of the notable seasonality of surface warming in this region to both land–surface–hydroclimate interactions and changes in winter circulation. In the lower stratosphere, a cooling trend is evident in all seasons, not unexpectedly, but a pronounced seasonality is again apparent, with the strongest cooling in summer. The near-zero trend tropopause region is a rare point of confluence for seasonal trends.*

RÉSUMÉ *[Traduit par la rédaction] Au cours du XXe siècle, le réchauffement de la surface des continents du nord a varié d'une saison à l'autre. Il est particulièrement prononcé dans le nord-ouest du Canada, où les tendances hivernales sont beaucoup plus marquées que les tendances estivales. Les tendances de température en altitude dans la région sont analysées dans trois ensembles de données de radiosondage de 1958 à 2012 afin d'évaluer leur structure saisonnière. La variation saisonnière des tendances en altitude peut fournir des indications sur les processus dynamiques et thermodynamiques à l'origine de ces tendances, y compris le réchauffement à la surface. L'accent n'est pas mis sur la structure canonique des tendances séculaires (c'est-à-dire à long terme) – réchauffement de la troposphère et refroidissement de la stratosphère –, mais sur sa variation saisonnière. Nous constatons que la différence de tendance entre l'hiver et l'été boréal dans le nord-ouest du Canada est positive et importante dans la basse troposphère (*$p \gtrsim$ *500 hPa) et la basse stratosphère (50 hPa* $\lesssim$ *p* $\lesssim$ *150 hPa); elle est plus importante à la surface et plus faible à la tropopause. La saisonnalité décroissante de la tendance troposphérique en fonction de l'altitude tend à confirmer l'attribution de la saisonnalité marquée du réchauffement de la surface dans cette région à la fois aux interactions entre la surface terrestre et l'hydroclimat et aux changements de la circulation hivernale. Dans la basse stratosphère, une tendance au refroidissement est évidente en toutes saisons, ce qui correspond aux prévisions, mais une saisonnalité prononcée est à nouveau apparente, avec un refroidissement plus prononcé en été. La zone de la tropopause à tendance quasi nulle est un rare point de confluence des tendances saisonnières.*

KEYWORDS temperature trends; observational analysis; troposphere; northwestern Canada; climate change

1 Introduction

The steep warming trend in surface air temperature (SAT) during recent decades and its origin are being actively investigated (DelSole et al., 2011; Stolpe et al., 2017). This trend is characterized by a lack of uniformity across seasons, as well as pronounced regional variations (Nigam et al., 2017). Previous studies have determined that the boreal winter trend relative to other seasons is notably large in mid- to high latitudes of the continents in the northern hemisphere (Nigam

†Current affiliation: Universities Space Research Association, Columbia, MD and Global Modeling and Assimilation Office, NASA GSFC, Greenbelt, MD
*Corresponding author's email: nigam@umd.edu

et al., 2017; Wallace et al., 2012). Specifically, Nigam et al. (2017) showed that seasonality in twentieth-century warming is particularly striking over northwestern North America and northern Eurasia, where winter trends are more than twice as large as summer ones.

This SAT seasonality over continents in the northern hemisphere is attributed to both dynamic and thermodynamic mechanisms. Dynamically, changes in boreal winter circulation and related thermal advection strengthen winter SAT trends (Stine et al., 2009; Wallace et al., 2012). Thermodynamically, an active hydrologic cycle in summer permits latent (i.e., evaporative) disposition of some of the additional radiative energy from rising greenhouse gas concentrations, reducing SAT trends in summer (Nigam et al., 2017). To further examine the relative roles of these mechanisms, this study seeks to characterize the seasonal structure of temperature trends in the atmospheric column above surface regions exhibiting large seasonality in warming. Does the seasonality of SAT trends continue into the troposphere and lower stratosphere, or is it largely a surface phenomenon?

The annual-mean temperature trend over recent decades is generally positive in the troposphere and negative in the stratosphere (Hartmann et al., 2013)—the canonical secular warming structure. The cooling trend in the lower stratosphere is well documented (Ramaswamy et al., 2001; Randel et al., 2009; Seidel et al., 2011) though radiosonde measurements indicate a reversal of this trend in the early twenty-first century (Philipona et al., 2018). The seasonal variation in stratospheric temperature trends has also been examined. In polar regions, strong springtime cooling and weak wintertime warming lead to large seasonality in stratospheric temperature trends (Ivy et al., 2016; Randel et al., 2009; Seidel et al., 2011; Thompson & Solomon, 2005). The seasonality is weaker in the tropical stratosphere, with minimal cooling in spring and maximum cooling in fall (Free, 2011; Fu et al., 2010; Thompson & Solomon, 2005). The seasonality in stratospheric trends has been attributed to both radiative and dynamic causes (Bohlinger et al., 2014). The strengthening (weakening) of the Brewer–Dobson circulation (Cohen et al., 2014) in boreal winter (spring) leads to enhanced (reduced) downwelling at high latitudes and thus less (more) stratospheric cooling (Fu et al., 2010; Ivy et al., 2016; Young et al., 2012). Ozone loss in summer is the main driver of summer cooling trends in polar regions (Ivy et al., 2016). Sea surface temperatures have also been implicated in stratospheric temperature trends. Garfinkel et al. (2015) found that about half of the spring cooling trend in the polar stratosphere could be attributed to sea surface temperature forcing.

Tropospheric temperature trends have also drawn attention, especially as to why they differ from surface temperature trends (Thorne et al., 2011). In the Tropics, warming is enhanced in the upper troposphere, around 300 hPa (Thorne et al., 2011), notwithstanding discussions on the level of agreement between observations and model simulations (Christy et al., 2010; Douglass et al., 2008; Santer et al., 2008). Screen et al. (2012) examined tropospheric warming in the Arctic, noting more pronounced warming in fall and winter than in spring and summer. Lanzante et al. (2003a) studied upper-tropospheric trends over the 1979–1997 period and found greater warming during fall for the northern hemisphere; these 19-year trends are not necessarily reflective of secular warming because of the potential aliasing of multidecadal natural variability in short period trends. Apart from a few regional studies on the seasonality of tropospheric trends (Gevorgyan, 2014; Kothawale & Singh, 2017; Zhang & Zhou, 2013), their seasonal structure in the northern extratropics remains largely undocumented.

The present study seeks to characterize the seasonality of the secular trend in upper-air temperatures over northern Canada, a region of pronounced seasonal variation in SAT trends (Nigam et al., 2017). The temperature trends during the 1958–2012 period are analyzed from the three radiosonde data products described in Section 2; the analysis method is outlined in Section 3. The boreal winter and summer trends in the troposphere and lower stratosphere, as well as their difference, are discussed in Section 4. Concluding remarks follow in Section 5.

2 Data

a *Upper-Air Data*

The present analysis, targeting upper-air temperature trends in this region is, of necessity, restricted to the post-International Geophysical Year (IGY; http://www.nasonline.org/about-nas/history/archives/milestones-in-NAS-history/the-igy.html) period (post-1958) when upper-air meteorological data began to be routinely collected. Upper-air data are often subject to instrumentation and measurement changes that can result in artificial temperature changes (Lanzante et al., 2003a). Therefore, in analyzing long-term trends in upper-air data, it is necessary to use homogenized datasets. Three such analyses of upper-air temperature are examined in this study, with a common period of 1958–2012. Although some raw input data are shared among them, they differ in the way they treat inhomogeneities, as described below. Although the goal was to use all available homogenized radiosonde data products (Hartmann et al., 2013), the Radiosonde Atmospheric Temperature Products for Assessing Climate dataset B (RATPAC-B) from the National Climatic Data Center (Free et al., 2005; Lanzante et al., 2003a, 2003b) was not used in this study because it does not contain any stations in the main region of interest.

1 HADAT2

The UK Met Office's Hadley Centre Atmospheric Temperature, version 2 (HadAT2) dataset (Thorne et al., 2005) provides monthly temperature anomalies for 850 hPa up to 50 hPa relative to the 1966–1995 climatology (Met Office, 2010). Data are available for 676 stations worldwide for the 1958–2012 period. This dataset uses comparisons with neighbouring stations to handle spatial and temporal inhomogeneities.

2 ITERATIVE UNIVERSAL KRIGING

The iterative universal kriging (IUK) Radiosonde Analysis Project (Sherwood & Nishant, 2015), version 2.01 is also analyzed. This dataset provides monthly temperature estimates for 527 stations worldwide for the 1960–2015 period (Climate Change Research Centre, 2016). This dataset handles inhomogeneities by applying temperatures measured at a station to a multiple regression model that includes instrument changes, trends, and natural variability (Sherwood & Nishant, 2015).

The HadAT2 and IUK datasets contain data at many of the same station locations. For this study, stations were excluded if they (i) were in coastal areas, (ii) were missing 10 or more years of data in either winter or summer, or (iii) were outside the region of maximum surface temperature trend seasonality in northwestern Canada (i.e., where the difference between near-surface temperature trends in winter and summer is approximately 0.5°C per decade). Thus, the five stations used in this study are Fort Nelson (WMO-71945), Fort Smith (WMO-71934), Whitehorse (WMO-71964), Norman Wells (WMO-71043), and The Pas (WMO-71867).

3 RAOBCORE-V1.5

The Radiosonde Observation Correction Using Reanalyses, version 1.5 (RAOBCORE-v1.5), dataset (Haimberger, 2007; Haimberger et al., 2012) provides adjusted temperature anomalies on a 10° resolution grid for the 1958–2014 period (RAOBCORE/RICH, 2015). This dataset reduces inhomogeneities by comparing temperatures with those from reanalysis background forecasts.

b *Reanalysis*

Circulation changes are analyzed using upper-air geopotential heights from the Twentieth Century Reanalysis, V2c (NOAA20CRv2c), produced by the National Oceanic and Atmospheric Administration (NOAA) (Compo et al., 2011), which is available at monthly resolution from January 1851 to December 2014 from the Physical Sciences Laboratory (2014).

c *Near-Surface Temperature Data*

Near-surface air temperature trends over continental regions are calculated using the monthly Climate Research Unit Time Series (CRU-TS), version 4.00 dataset (Harris et al., 2014). This dataset is available on a 0.5° continental grid for January 1901 to December 2015 from the University of East Anglia (Climate Research Unit, 2017).

3 Methods

Seasonal data are analyzed following boreal season definitions (i.e., winter is the average of December, January, and February (DJF), and summer is the average of June, July, and August (JJA)). Linear trends are computed from linear least squares regression. The average trends over multiple stations were computed by taking the trend of the average seasonal temperature from the stations. We found that reversing this computation (i.e., taking the average of the individual seasonal trends from each station) yielded minimal differences.

Statistical significance of trends was estimated at confidence levels from the ratio of the slope and its standard error, accounting for temporal autocorrelation in the temperature time series by using an effective sample size in both the computation of the standard error and in the indexing of the critical *t*-value (Santer et al., 2000). We assume the seasonal time series to be first-order autoregressive (AR(1)). Significance is noted at both the 95% and 90% confidence levels in this study. Statistical significance of trend differences was estimated by determining whether the trend in the difference time series is significantly different from zero at a given confidence level, as in Santer et al. (2000).

4 Results

a *Seasonality of Surface Temperature Trends over North America*

The pronounced seasonality in the twentieth century (1902–2014) SAT trends, especially over North America and parts of Eurasia, is extensively documented in Nigam et al. (2017). The focus here is on the region in northwestern Canada where the seasonality in SAT trends is particularly robust. On a century-long time scale, this seasonality in secular surface warming was attributed to land–surface–hydroclimate interactions and changes in low-level atmospheric circulation. At the surface in this mid- to high-latitude region, the hydrologic cycle is active in summer and dormant in winter. The positive trend in summer evapotranspiration in this region, as documented in Nigam et al. (2017), leads to the latent disposition of energy and, hence, summer temperature trends that are reduced relative to other seasons. Furthermore, the secular change in low-level atmospheric circulation and related thermal advection simultaneously leads to increased winter trends in this region (Nigam et al., 2017; Wallace et al., 2012). The seasonality in surface warming over northwestern Canada is thus consistent with both thermodynamically reduced summer trends and dynamically increased winter trends.

It is instructive to examine whether the linear SAT trends in the comparatively shorter (post-IGY) period continue to exhibit the large seasonality over the northern continents highlighted in Nigam et al. (2017). Figure 1 displays the winter-minus-summer difference in SAT trends in this period from the CRU-TS4.00 data. Over this shorter (58-year) period, northwestern North America has warmed more in winter, as evident from the large winter–summer trend difference (as much as 0.5°C per decade). A comparison with Nigam et al. (2017; Fig. 3, top-right panel) shows that

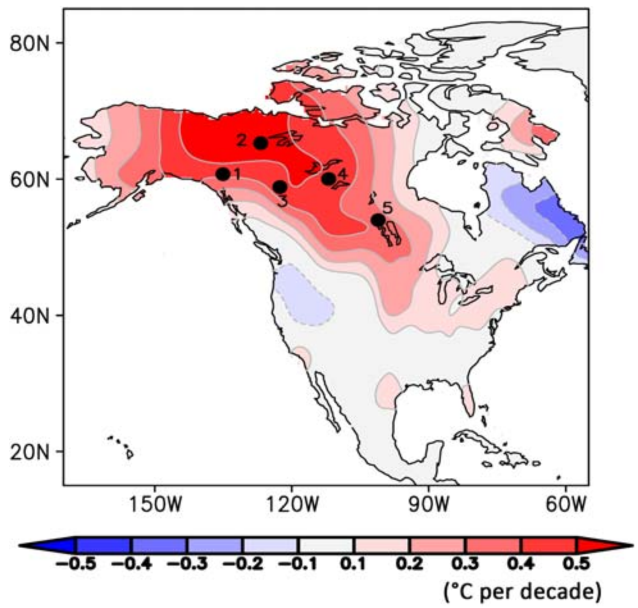

Fig. 1 Difference between the winter and summer temperature trends in the 0.5° resolution CRU-TS4.00 surface air temperature (SAT) over North America during the 1958–2015 period. Contour interval and shading threshold is 0.1°C per decade. The fields are shown after nine applications of the 9-point smoother (smth9) in the Grid Analysis and Display System (GrADS). The black dots mark the locations of the five radiosonde stations analyzed in this study: Whitehorse (1; WMO#71964), Norman Wells (2; WMO#71043), Fort Nelson (3; WMO#71945), Fort Smith (4; WMO #71934), and The Pas (5; WMO#71867).

the trend seasonality is, if anything, more intense in the shorter period.

b *Vertical Structure of Seasonal Temperature Trends*

The investigation of upper-air temperature trends begins with the analysis of radiosonde soundings. Five stations located within the region of interest are marked with black dots in Fig. 1. Both the HadAT2 and IUK datasets have data at these stations, as noted in Section 2. Figure 2 shows the vertical profile of winter and summer temperature trends at each station from both datasets.

A common feature of temperature trends based on radiosonde data is the stronger surface warming in winter at all stations, consistent with Nigam et al. (2017). The HadAT2 and IUK analyses exhibit some notable differences. At station 71945, winter (summer) temperature trends are negative (positive) from 300 hPa to 100 hPa in IUK but quite the opposite in HadAT2; also, summer trends are negative near the surface in the IUK analysis at stations 71945 and 71934 but this is not seen in the HadAT2 analysis. Still, the two analyses agree on the main features: stronger winter warming at the surface, with the warming decreasing upwards through the troposphere and cooling in the lower stratosphere.

Figure 3 shows the vertical profile of the seasonal temperature trends, averaged over the five stations; HadAT2 data are analyzed because they are available at all five stations. The trend at the surface is positive in all four seasons, with a winter–summer difference of approximately 0.4°C per decade consistent with the estimate from the independent CRU-TS4.00 analysis (Fig. 1). Winter trends are greater than summer ones through the entire column extending from the land surface to the lower stratosphere; the two are closest at 300 hPa, near the tropopause, where all four seasonal trends are within 0.1°C per decade of each other. The winter-minus-summer temperature trends have a similar vertical structure in the HadAT2 (thick black line) and IUK analysis (dashed black line): strongest at the surface and decreasing through the troposphere.

In the lower stratosphere, trends become negative and the seasonality resumes, with strong cooling in all seasons except winter. Note that displayed summer trends are not significant in the mid-troposphere (200 and 300 hPa), and winter trends are only significant at pressure levels above 200 hPa. The difference between winter and summer trends (black line in Fig. 3) is statistically significant at the 95% level only at 850, 700, and 50 hPa. Thus, although the winter trend is greater than the summer one throughout the entire column, their difference is only statistically significant near the surface and in the lower stratosphere.

To confirm that the identified seasonal trends are linear and not overly influenced by any discrete event during the time period, Fig. 4 shows the time series of boreal winter and summer temperatures averaged over the five HadAT2 stations in the mid-stratosphere (Fig. 4a) and near the surface (Fig. 4b). To confirm that these five stations can be averaged to determine the regional time series of temperature, correlation coefficients were computed between each station. Average correlations between stations were 0.84, 0.91, 0.72, and 0.39 for 50 hPa winter temperature, 50 hPa summer temperature, 850 hPa winter temperature, and 850 hPa summer temperature, respectively. Figure 4 shows that winter temperatures are characterized by greater interannual variability than summer temperatures, as noted before (Stine et al., 2009). As seen earlier (Fig. 3), winter temperature trends are positive near the surface (Fig. 4b) and weakly negative in the lower stratosphere (Fig. 4a). Summer trends are weakly positive near the surface (Fig. 4b) and strongly negative in the lower stratosphere (Fig. 4a). Importantly, the significant trends identified in Fig. 3 are confirmed to be linear from these time series.

The lower stratospheric temperature trends observed in this region are in general accord with previous analyses. The relatively weak winter cooling is consistent with the findings on high-latitude stratospheric temperature trends (Bohlinger et al., 2014; Ivy et al., 2016; Thompson & Solomon, 2005). Earlier studies have found changes in the strength of the Brewer–Dobson circulation (BDC) to be a primary cause of the winter trends. The annual-mean BDC is shown to have strengthened over recent decades (Fu et al., 2015) as a result of greenhouse-gas-induced warming of the tropical troposphere and subsequent increases in meridional temperature gradient, westerly zonal winds, and wave driving in the

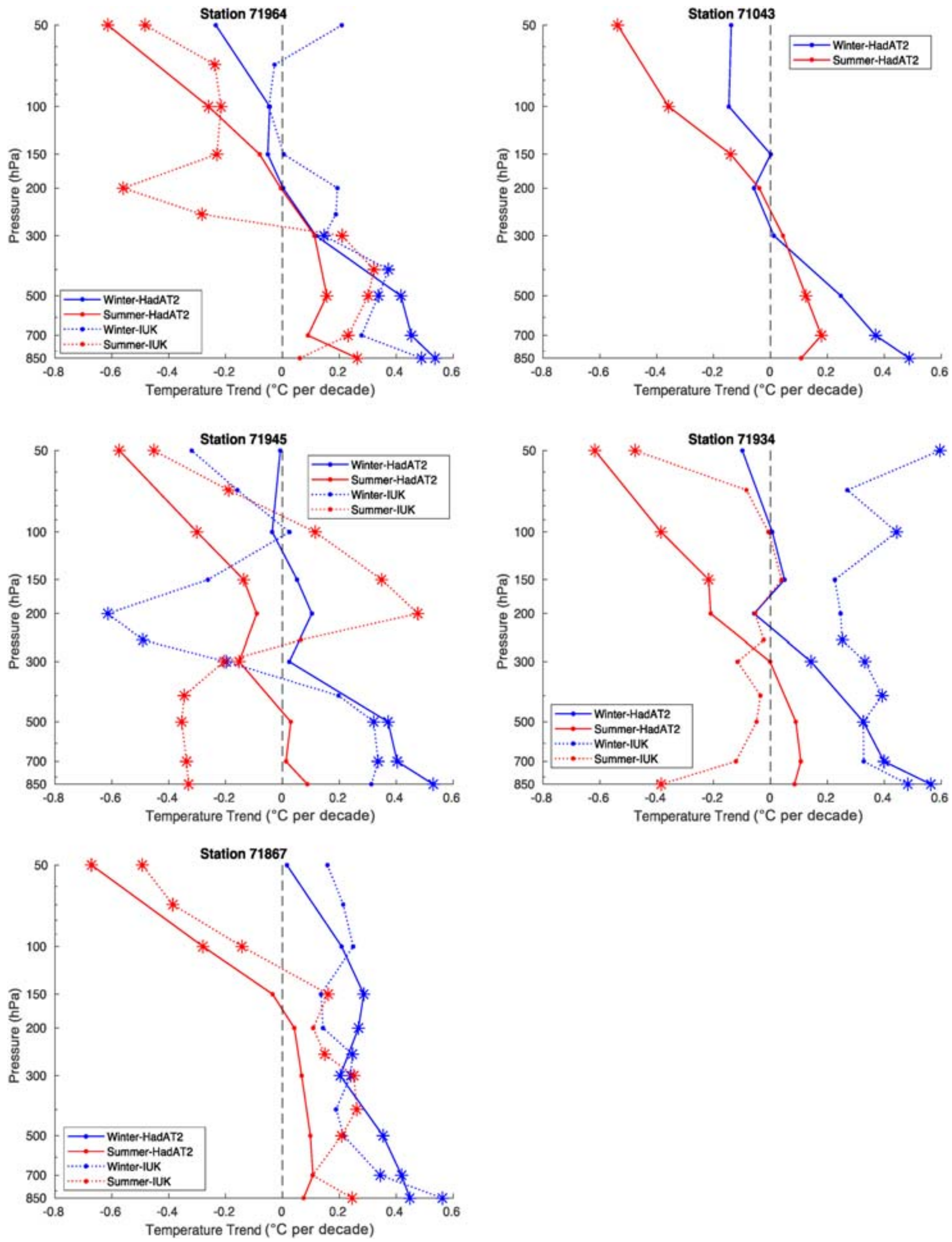

Fig. 2 Winter (blue) and summer (red) temperature trends over the 1960–2012 period for HadAT2 (solid lines) and IUK (dotted lines) at the five individual station locations plotted in Fig. 1; note, IUK does not have data at station 71043. Trends significant at the 95% level are denoted by star symbols.

tropical lower stratosphere (Eichelberger & Hartmann, 2005; Garcia & Randel, 2008). In the northern hemisphere, the strengthening of the BDC is most pronounced in winter, but there is a slight weakening trend in spring (Fu et al., 2010; Li et al., 2008; McLandress & Shepherd, 2009). The intensified winter BDC leads to increased downwelling at high latitudes and, hence, reduced stratospheric cooling.

Radiative effects due to ozone variations have also been shown to influence stratospheric temperatures. The seasonal cycle of ozone is fairly muted at high latitudes (compared with the Tropics) but with slightly higher values in late winter and early spring (Hassler et al., 2013). Ozone depletion, the long-term decline in ozone concentration, leads to cooling in the stratosphere. The depletion is attributable to the same halogen chemistry mechanisms that led to the Antarctic ozone hole although the warmer Arctic and the larger influence of dynamics in the northern hemisphere prevent losses of the same magnitude (Solomon et al., 2014).

The analysis is complicated by the link between the dynamic and radiative processes controlling stratospheric temperatures: increased downwelling over the Arctic resulting from a strengthening BDC also leads to greater ozone transport into high latitudes and, hence, radiative heating (Bednarz et al., 2016). Figure 3 indicates that in this particular region of northwestern Canada, the dynamic warming potentially associated with the strengthened BDC is the main

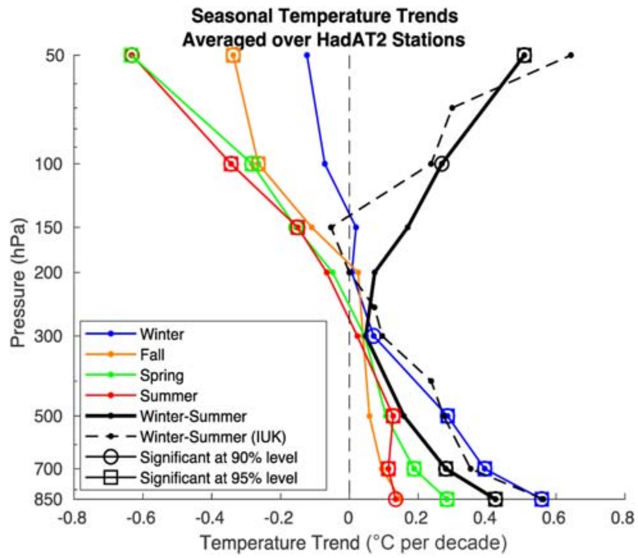

Fig. 3 The linear trend in seasonal temperatures (°C per decade) at various vertical levels in the troposphere and lower stratosphere, averaged over the five HadAT2 stations marked by black dots in Fig. 1. Trends are for the 1958–2012 period. Trends (and trend differences, in the case of winter-minus-summer difference, black line) significant at the 90% (95%) confidence level are indicated with open circles (squares). For comparison, the winter-minus-summer trend difference is also shown for the IUK data (dashed black line) averaged over four stations (see Fig. 2).

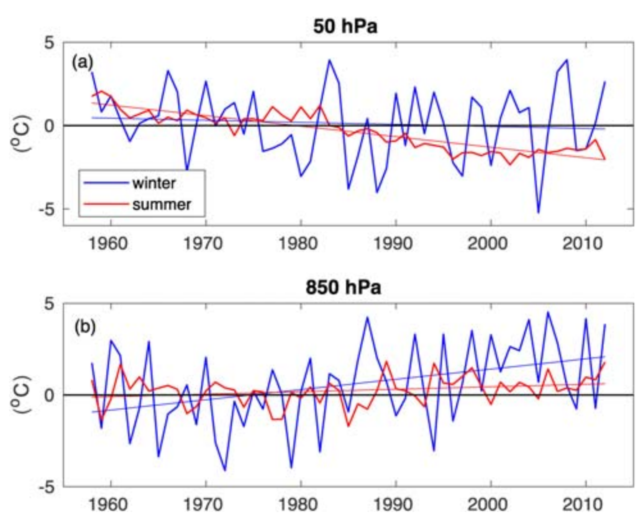

Fig. 4 Time series of winter (blue) and summer (red) temperature anomalies (°C) over the 1958–2012 period for 50 hPa (top) and 850 hPa (bottom) averaged over the five HadAT2 stations marked in Fig. 1. Thin straight lines indicate the linear fits to the time series.

control on the stratospheric winter temperature trends, while summer and fall experience sufficiently strong radiative cooling from ozone depletion to compensate for any dynamically induced warming. In spring, the weakening BDC (Fu et al., 2010) and the peak in ozone depletion (Ivy et al., 2016) combine to generate strong cooling trends.

Unlike the lower stratosphere, where the seasonal variation of high-latitude temperature trends is well studied, tropospheric temperature trends, especially their seasonality, is only now receiving attention; they are the focus of the following subsection.

c *Seasonal Distribution of Tropospheric Temperature Trends over North America*

The RAOBCORE-v1.5 radiosonde temperature dataset is used to analyze the three-dimensional structure of tropospheric temperature trends. The horizontal distribution of the winter-minus-summer difference in temperature trends over the North American continent is displayed in Fig. 5 at various vertical levels. The bottom panel shows the seasonal difference in 850 hPa trends, which is similar in structure and amplitude to the surface difference (Fig. 1), notably, over northwestern Canada. Moving upwards into the mid-troposphere (500 hPa), the region showing large winter-minus-summer difference in trends (i.e., maximum seasonality in trends) remains over northwestern Canada, albeit with diminished amplitude relative to the surface. Near the tropopause (300 hPa), the winter-minus-summer difference in temperature trends is much weaker over the entire continent, including northwestern Canada, consistent with Fig. 3.

The reduction in the seasonality (i.e., winter-minus-summer difference) of temperature trends as one moves away from the surface into the mid-troposphere over northwestern Canada is due to the weakening of the winter trend; the summer trend does not change much with height (see Fig. 3). Previous work has attributed the relatively strong winter trends in this region to circulation changes (Wallace et al., 2012). Figure 6 shows the trends in geopotential height at 850 and 300 hPa from the NOAA20CRv2c reanalysis, with the HadAT2 station locations indicated by red dots. Geostrophic circulation trends, inferred from geopotential height trends, show that the 850 hPa winter circulation trends over the 1958–2012 period led to the onshore advection of warmer marine air into northwestern Canada, enhancing near-surface warming trends in winter. As expected, circulation trends are much weaker in summer. The winter-minus-summer trends in 850 hPa circulation (Fig. 6, bottom-right panel), reflecting mostly the winter trends (Fig. 6, bottom-left panel), contributed to the strong seasonality in temperature trends in the region, as shown in Fig. 5. Although this circulation-trend pattern continues upwards into the troposphere (Fig. 6, top panels), the climatological land–ocean temperature contrast weakens significantly with increasing height, with little trace above the mid-troposphere. The winter temperature trends over northwestern Canada are thus dynamically strengthened in the lower to mid-troposphere but not in the upper troposphere.

5 Conclusions

This analysis is a continuation of the authors' efforts (Nigam et al., 2017) to expand the characterization of the secular

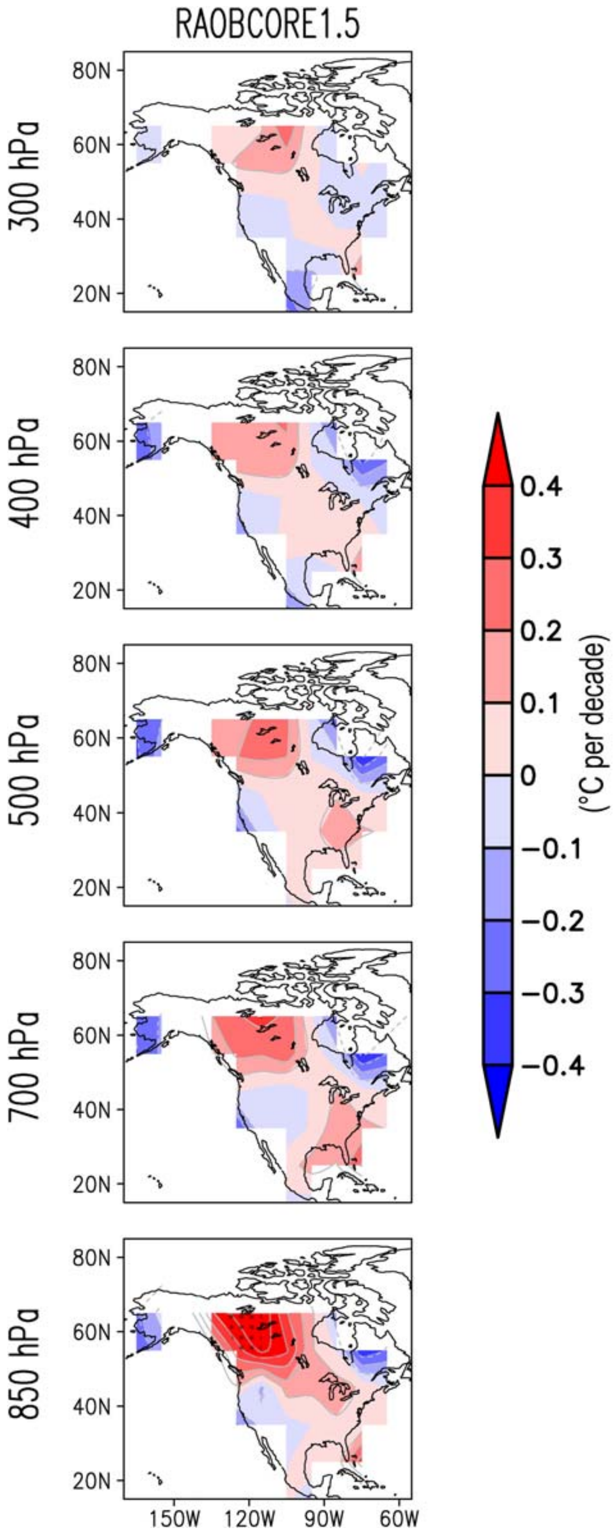

Fig. 5 Winter-minus-summer trends in temperature (°C per decade) over the 1958–2012 period from the 10° resolution RAOBCORE-v1.5 adjusted temperature anomaly. The contour and shading interval is 0.1°C per decade. Trend differences are shown at the 300 hPa (top), 400 hPa (second from top), 500 hPa (middle), 700 hPa (second from bottom), and 850 hPa (bottom) levels. The fields are displayed after nine applications of the 9-point smoother (smth9) in GrADS. The black dots indicate trend differences significant at the 95% level.

change signal in atmospheric temperature, especially its seasonality, which is large at the surface of the northern continents. The analysis differs from that of Nigam et al. (2017) because of its focus on upper-air temperature trends. The secular change signal in tropospheric and lower stratospheric temperature over northwestern North America—a focal point of the notable seasonality in SAT trends (Nigam et al., 2017)—is analyzed from radiosonde soundings and atmospheric reanalysis. A key motivation for this analysis is the continued assessment of the viability of the hypotheses advanced for the seasonality in SAT trends (Nigam et al., 2017; Stine et al., 2009; Wallace et al., 2012). In the region of the largest winter-minus-summer difference in surface temperature trends (northwestern Canada), the following can be shown:

- The seasonality in trends diminishes with altitude, becoming a minimum at the tropopause and increasing again in the lower stratosphere. The difference between winter and summer temperature trends is statistically significant in the lower troposphere and lower stratosphere.
- In the lower stratosphere, cooling trends are found in all seasons but the winter trends are warmer than others (which closely track each other), consistent with the findings of Ivy et al. (2016). The seasonality in stratospheric temperature trends is well documented and attributed to ozone depletion and changes in the strength of the BDC (Fu et al., 2010; Ivy et al., 2016), with different contributions from each in different seasons.
- In the lower troposphere, the strong seasonality is consistent with the thermodynamic suppression of summer warming trends (from evaporative disposition of the additional radiative energy incident at the surface—a mechanism advanced by Nigam et al. (2017)) and the dynamic strengthening of winter warming trends (from circulation-trend induced thermal advection (e.g., Wallace et al., 2012)). The vertical structure of seasonal temperature trends in the troposphere offers support for both mechanisms. The attenuation of winter trends with height reflects the presence of a dynamic component (as moving upwards from a level of strong land–sea contrast would lead to diminished thermal advection), while the weak variation of summer trends with height (trends approximately 0.1°C per decade up to 500 hPa) is consistent with the absence of a dynamic component (due to much weaker circulation trends in summer).

Natural variability can also contribute to these trends (and, perhaps, even to their winter-minus-summer differences), and the separation of natural and anthropogenically forced components in these 55-year trends would be worthwhile. The possibility of multidecadal natural variability becoming aliased into linear trends is considered in the context of SAT trends in Nigam et al. (2017, see Section 4c and Appendix A). Interestingly, however, the 55-year linear trends documented here exhibit a winter–summer difference at the surface that is similar to that present in the century-long

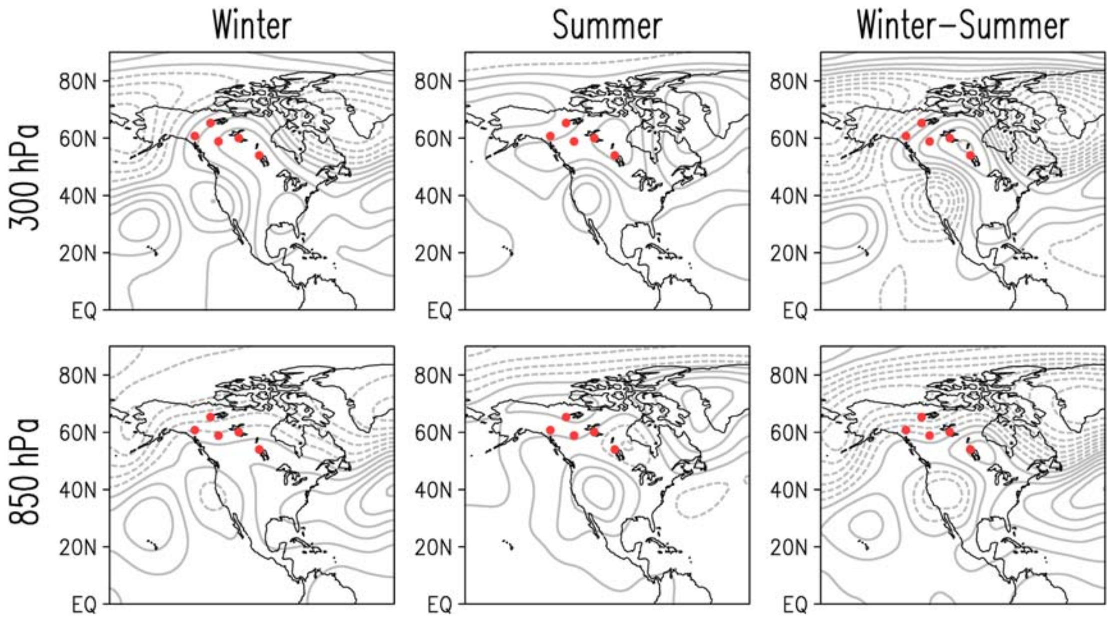

Fig. 6 Winter (left), summer (middle), and winter-minus-summer (right) trends in geopotential height (m per decade) over the 1958–2012 period from the NOAA20CRv2c reanalysis. Trends are shown at 300 hPa (top) and 850 hPa (bottom). The contour interval is 1 m per decade for 850 hPa and 2 m per decade for 300 hPa. Red dots indicate the locations of the HadAT2 stations analyzed in this study. The fields are displayed after nine applications of the 9-point smoother (smth9*)* in GrADS.

trends reported in Nigam et al. (2017). Further elucidation of the mechanisms generating the seasonality in surface and upper-air temperature trends will require a comprehensive analysis of the surface energy balance and the regional atmospheric and terrestrial water cycles.

Acknowledgements

The authors thank Dr. Alfredo Ruiz-Barradas for his help with datasets and analysis techniques.

Disclosure statement

No potential conflict of interest was reported by the author(s).

Funding

Vishal Ravi's research internship during the summer of 2016 was supported by the Research Experiences for Undergraduates (REU) funds on the National Science Foundation (NSF) Award [AGS1439940]. Natalie Thomas's doctoral studies (2015–2018) at the University of Maryland were supported by a National Defense Science and Engineering Graduate (NDSEG) Fellowship.

ORCID

Sumant Nigam http://orcid.org/0000-0002-9668-2979

References

Bednarz, E. M., Maycock, A. C., Abraham, N. L., Braesicke, P., Dessens, O., & Pyle, J. A. (2016). Future Arctic ozone recovery: The importance of chemistry and dynamics. *Atmospheric Chemistry and Physics*, *16*(18), 12159–12176. https://doi.org/10.5194/acp-16-12159-2016

Bohlinger, P., Sinnhuber, B. M., Ruhnke, R., & Kirner, O. (2014). Radiative and dynamical contributions to past and future Arctic stratospheric temperature trends. *Atmospheric Chemistry and Physics*, *14*(3), 1679–1688. https://doi.org/10.5194/acp-14-1679-2014

Christy, J. R., Herman, B., Pielke Sr., R., Klotzbach, P., McNider, R. T., Hnilo, J. J., Spencer, R. W., Chase, T., & Douglass, D. (2010). What do observational datasets say about modeled tropospheric temperature trends since 1979? *Remote Sensing*, *2*(9), 2148–2169. https://doi.org/10.3390/rs2092148

Climate Change Research Centre. (2016). *IUK Radiosonde Analysis Project – now updated through* 2015. University of New South Wales. http://web.science.unsw.edu.au/~stevensherwood/radproj/index.html

Climate Research Unit. (2017). *CRU TS* (Version 4.00) [Dataset]. University of East Anglia. https://crudata.uea.ac.uk/cru/data/hrg/cru_ts_4.00/

Cohen, N. Y., Gerber, E. P., & Buhler, O. (2014). What drives the Brewer-Dobson circulation? *Journal of the Atmospheric Sciences*, *71*(10), 3837–3855. https://doi.org/10.1175/jas-d-14-0021.1

Compo, G. P., Whitaker, J. S., Sardeshmukh, P. D., Matsui, N., Allan, R. J., Yin, X., Gleason, B. E., Vose, R. S., Rutledge, G., Bessemoulin, P., Brönnimann, S., Brunet, M., Crouthamel, R. I., Grant, A. N., Groisman, P. Y., Jones, P. D., Kruk, M. C., Kruger, A. C., Marshall, G. J., … Worley, S. J. (2011). The twentieth century reanalysis project. *Quarterly Journal of the Royal Meterological Society*, *137*(654), 1–28. https://doi.org/10.1002/qj.776

DelSole, T., Tippett, M. K., & Shukla, J. (2011). A significant component of unforced multidecadal variability in the recent acceleration of global warming. *Journal of Climate*, *24*(3), 909–926. https://doi.org/10.1175/2010jcli3659.1

Douglass, D. H., Christy, J. R., Pearson, B. D., & Singer, S. F. (2008). A comparison of tropical temperature trends with model predictions. *International Journal of Climatology*, *28*(13), 1693–1701. https://doi.org/10.1002/joc.1651

Eichelberger, S. J., & Hartmann, D. L. (2005). Changes in the strength of the Brewer-Dobson circulation in a simple AGCM. *Geophysical Research Letters*, *32*(15), L15807. https://doi.org/10.1029/2005gl022924

Free, M. (2011). The seasonal structure of temperature trends in the tropical lower stratosphere. *Journal of Climate*, *24*(3), 859–866. https://doi.org/10.1175/2010jcli3841.1

Free, M., Seidel, D. J., Angell, J. K., Lanzante, J., Durre, I., & Peterson, T. C. (2005). Radiosonde atmospheric temperature products for assessing Climate (RATPAC): A new data set of large-area anomaly time series. *Journal of Geophysical Research-Atmospheres*, *110*(D22), D22101. https://doi.org/10.1029/2005jd006169

Fu, Q., Lin, P., Solomon, S., & Hartmann, D. L. (2015). Observational evidence of strengthening of the Brewer-Dobson circulation since 1980. *Journal of Geophysical Research-Atmospheres*, *120*(19), 10214–10228. https://doi.org/10.1002/2015jd023657

Fu, Q., Solomon, S., & Lin, P. (2010). On the seasonal dependence of tropical lower-stratospheric temperature trends. *Atmospheric Chemistry and Physics*, *10*(6), 2643–2653. https://doi.org/10.5194/acp-10-2643-2010

Garcia, R. R., & Randel, W. J. (2008). Acceleration of the Brewer-Dobson circulation due to increases in greenhouse gases. *Journal of the Atmospheric Sciences*, *65*(8), 2731–2739. https://doi.org/10.1175/2008jas2712.1

Garfinkel, C. I., Hurwitz, M. M., & Oman, L. D. (2015). Effect of recent sea surface temperature trends on the Arctic stratospheric vortex. *Journal of Geophysical Research-Atmospheres*, *120*(11), 5404–5416. https://doi.org/10.1002/2015jd023284

Gevorgyan, A. (2014). Surface and tropospheric temperature trends in Armenia. *International Journal of Climatology*, *34*(13), 3559–3573. https://doi.org/10.1002/joc.3928

Haimberger, L. (2007). Homogenization of radiosonde temperature time series using innovation statistics. *Journal of Climate*, *20*(7), 1377–1403. https://doi.org/10.1175/jcli4050.1

Haimberger, L., Tavolato, C., & Sperka, S. (2012). Homogenization of the global radiosonde temperature dataset through combined comparison with reanalysis background series and neighboring stations. *Journal of Climate*, *25*(23), 8108–8131. https://doi.org/10.1175/jcli-d-11-00668.1

Harris, I., Jones, P. D., Osborn, T. J., & Lister, D. H. (2014). Updated high-resolution grids of monthly climatic observations - the CRU TS3.10 dataset. *International Journal of Climatology*, *34*(3), 623–642. https://doi.org/10.1002/joc.3711

Hartmann, D. L., Klein Tank, A. M. G., Rusticucci, M., Alexander, L. V., Brönnimann, S., Charabi, Y., Dentener, F. J., Dlugokencky, E. J., Easterling, D. R., Kaplan, A., Soden, B. J., Thorne, P. W., Wild, M., & Zhai, P. M. (2013). Observations: Atmosphere and surface. In T. F. Stocker, D. Qin, G.-K. Plattner, M. Tignor, S. K. Allen, J. Boschung, A. Nauels, Y. Xia, V. Bex, & P. M. Midgley (Eds.), *Climate change 2013: The physical science basis. Contribution of Working Group I to the Fifth assessment Report of the Intergovernmental Panel on Climate Change* (pp. 159–254). Cambridge University Press.

Hassler, B., Young, P. J., Portmann, R. W., Bodeker, G. E., Daniel, J. S., Rosenlof, K. H., & Solomon, S. (2013). Comparison of three vertically resolved ozone data sets: Climatology, trends and radiative forcings. *Atmospheric Chemistry and Physics*, *13*(11), 5533–5550. https://doi.org/10.5194/acp-13-5533-2013

Ivy, D. J., Solomon, S., & Rieder, H. E. (2016). Radiative and dynamical influences on polar stratospheric temperature trends. *Journal of Climate*, *29*(13), 4927–4938. https://doi.org/10.1175/jcli-d-15-0503.1

Kothawale, D. R., & Singh, H. N. (2017). Recent trends in tropospheric temperature over India during the period 1971-2015. *Earth and Space Science*, *4*(5), 240–246. https://doi.org/10.1002/2016ea000246

Lanzante, J. R., Klein, S. A., & Seidel, D. J. (2003a). Temporal homogenization of monthly radiosonde temperature data. Part I: Methodology. *Journal of Climate*, *16*(2), 224–240. https://doi.org/10.1175/1520-0442(2003)016<0224:thomrt>2.0.co;2

Lanzante, J. R., Klein, S. A., & Seidel, D. J. (2003b). Temporal homogenization of monthly radiosonde temperature data. Part II: Trends, sensitivities, and MSU comparison. *Journal of Climate*, *16*(2), 241–262. https://doi.org/10.1175/1520-0442(2003)016<0241:thomrt>2.0.co;2

Li, F., Austin, J., & Wilson, J. (2008). The strength of the Brewer-Dobson circulation in a changing climate: Coupled chemistry-climate model simulations. *Journal of Climate*, *21*(1), 40–57. https://doi.org/10.1175/2007jcli1663.1

McLandress, C., & Shepherd, T. G. (2009). Simulated anthropogenic changes in the Brewer-Dobson circulation, including its extension to high latitudes. *Journal of Climate*, *22*(6), 1516–1540. https://doi.org/10.1175/2008jcli2679.1

Met Office. (2010). *Met Office Hadley Centre observations datasets* [Data set]. Retrieved 2016 from https://www.metoffice.gov.uk/hadobs/hadat/hadat2.html

Nigam, S., Thomas, N. P., Ruiz-Barradas, A., & Weaver, S. J. (2017). Striking seasonality in the secular warming of the northern continents: Structure and mechanisms. *Journal of Climate*, *30*(16), 6521–6541. https://doi.org/10.1175/jcli-d-16-0757.1

Philipona, R., Mears, C., Fujiwara, M., Jeannet, P., Thorne, P., Bodeker, G., Haimberger, L., Hervo, M., Popp, C., Romanens, G., Steinbrecht, W., Stübi, R., & Van Malderen, R. (2018). Radiosondes show that after decades of cooling, the lower stratosphere is now warming. *Journal of Geophysical Research - Atmospheres*, *123*(22), 12509–12522. https://doi.org/10.1029/2018JD028901

Physical Sciences Laboratory. (2014). *NOAA-CIRES Twentieth Century Reanalysis (V2c): Summary* [Dataset]. National Oceanic and Atmospheric Administration. https://psl.noaa.gov/data/gridded/data.20thC_ReanV2c.html

Ramaswamy, V., Chanin, M. L., Angell, J., Barnett, J., Gaffen, D., Gelman, M., Keckhut, P., Koshelkov, Y., Labitzke, K., Lin, J-JR, O'Neill, A., Nash, J., Randel, W., Rood, R., Shine, K., Shiotani, M., & Swinbank, R. (2001). Stratospheric temperature trends: Observations and model simulations. *Reviews of Geophysics*, *39*(1), 71–122. https://doi.org/10.1029/1999rg000065

Randel, W. J., Shine, K. P., Austin, J., Barnett, J., Claud, C., Gillett, N. P., Keckhut, P., Langematz, U., Lin, R., Long, C., Mears, C., Miller, A., Nash, J., Seidel, D. J., Thompson, D. W. J., Wu, F., & Yoden, S. (2009). An update of observed stratospheric temperature trends. *Journal of Geophysical Research-Atmospheres*, *114*(D2), D02107. https://doi.org/10.1029/2008jd010421

RAOBCORE/RICH (Version 1.5.1.) [Computer software]. (2015). https://www.univie.ac.at/theoret-met/research/raobcore/

Santer, B. D., Thorne, P. W., Haimberger, L., Taylor, K. E., Wigley, T. M. L., Lanzante, J. R., Solomon, S., Free, M., Gleckler, P. J., Jones, P. D., Karl, T. R., Klein, S. A., Mears, C., Nychka, D., Schmidt, G. A., Sherwood, S. C., & Wentz, F. J. (2008). Consistency of modelled and observed temperature trends in the tropical troposphere. *International Journal of Climatology*, *28*(13), 1703–1722. https://doi.org/10.1002/joc.1756

Santer, B. D., Wigley, T. M. L., Boyle, J. S., Gaffen, D. J., Hnilo, J. J., Nychka, D., Parker, D. E., & Taylor, K. E. (2000). Statistical significance of trends and trend differences in layer-average atmospheric temperature time series. *Journal of Geophysical Research-Atmospheres*, *105*(D6), 7337–7356. https://doi.org/10.1029/1999jd901105

Screen, J. A., Deser, C., & Simmonds, I. (2012). Local and remote controls on observed Arctic warming. *Geophysical Research Letters*, *39*(10), L10709. https://doi.org/10.1029/2012gl051598

Seidel, D. J., Gillett, N. P., Lanzante, J. R., Shine, K. P., & Thorne, P. W. (2011). Stratospheric temperature trends: Our evolving understanding. *Wiley Interdisciplinary Reviews-Climate Change*, *2*(4), 592–616. https://doi.org/10.1002/wcc.125

Sherwood, S. C., & Nishant, N. (2015). Atmospheric changes through 2012 as shown by iteratively homogenized radiosonde temperature and wind data (IUKv2). *Environmental Research Letters*, *10*(5), 054007. https://doi.org/10.1088/1748-9326/10/5/054007

Solomon, S., Haskins, J., Ivy, D. J., & Min, F. (2014). Fundamental differences between Arctic and Antarctic ozone depletion. *Proceedings of the National Academy of Sciences of the United States of America*, *111*(17), 6220–6225. https://doi.org/10.1073/pnas.1319307111

Stine, A. R., Huybers, P., & Fung, I. Y. (2009). Changes in the phase of the annual cycle of surface temperature. *Nature*, *457*(7228), 435–440. https://doi.org/10.1038/nature07675

Stolpe, M. B., Medhaug, I., & Knutti, R. (2017). Contribution of Atlantic and Pacific multidecadal variability to twentieth-century temperature changes. *Journal of Climate*, *30*(16), 6279–6295. https://doi.org/10.1175/jcli-d-16-0803.1

Thompson, D. W. J., & Solomon, S. (2005). Recent stratospheric climate trends as evidenced in radiosonde data: Global structure and tropospheric linkages. *Journal of Climate*, *18*(22), 4785–4795. https://doi.org/10.1175/jcli3585.1

Thorne, P. W., Lanzante, J. R., Peterson, T. C., Seidel, D. J., & Shine, K. P. (2011). Tropospheric temperature trends: History of an ongoing controversy. *Wiley Interdisciplinary Reviews-Climate Change*, *2*(1), 66–88. https://doi.org/10.1002/wcc.80

Thorne, P. W., Parker, D. E., Tett, S. F. B., Jones, P. D., McCarthy, M., Coleman, H., & Brohan, P. (2005). Revisiting radiosonde upper air temperatures from 1958 to 2002. *Journal of Geophysical Research-Atmospheres*, *110*(D18), D18105. https://doi.org/10.1029/2004jd005753

Wallace, J. M., Fu, Q., Smoliak, B. V., Lin, P., & Johanson, C. M. (2012). Simulated versus observed patterns of warming over the extratropical northern hemisphere continents during the cold season. *Proceedings of the National Academy of Sciences of the United States of America*, *109* (36), 14337–14342. https://doi.org/10.1073/pnas.1204875109

Young, P. J., Rosenlof, K. H., Solomon, S., Sherwood, S. C., Fu, Q., & Lamarque, J. F. (2012). Changes in stratospheric temperatures and their implications for changes in the Brewer Dobson circulation, 1979-2005. *Journal of Climate*, *25*(5), 1759–1772. https://doi.org/10.1175/2011jcli4048.1

Zhang, L. X., & Zhou, T. J. (2013). A comparison of tropospheric temperature changes over China revealed by multiple data sets. *Journal of Geophysical Research-Atmospheres*, *118*(10), 4217–4230. https://doi.org/10.1002/jgrd.50370